ACS OMEGA

Article

Cite This: ACS Omega 2018, 3, 11710−11717

http://pubs.acs.org/journal/acsodf

Experimental and Theoretical Investigations of Different Diketopyrrolopyrrole-Based Polymers

Pachaiyappan Murugan,[†] Venkatraman. Raghavendra,[‡,∥] Sundaresan Chithiravel,[§,∥] Kothandam Krishnamoorthy,[§,∥] Asit Baran Mandal,[†,⊥] Venkatesan Subramanian,*[,‡,∥] and Debasis Samanta*[,†,∥]

[†]Polymer Science & Technology Division and [‡]Inorganic and Physical Chemistry Department and Centre for High Computing, CSIR-CLRI, Adyar, Chennai 600020, India

[§]CSIR-NCL, Pune 411008, India

[∥]Academy of Scientific and Innovative Research, Gaziabad 201002, India

[⊥]CSIR-CGCRI, Kolkata 700032, India

Supporting Information

ABSTRACT: Diketopyrrolopyrrole (DPP)-based polymers are often considered as the most promising donor moiety in traditional bulk heterojunction solar cell devices. In this paper, we report the synthesis, characterization of various DPP-based copolymers with different molecular weights, and polydispersity where other aromatic repeating units (phenyl or thiophene based) are connected by alternate double bonds or triple bonds. Some of the copolymers were used for device fabrication and the crucial parameters such as fill factor (FF) and open circuit voltage (V_{oc}) were calculated. The density functional theory was used to optimize the geometries and deduce highest occupied molecular orbital−lowest unoccupied molecular orbital gaps of all the polymers and theoretically predict their optical and electronic properties. Optical properties of all the polymers, electrochemical properties, and band gaps were also obtained experimentally and compared with the theoretically predicted values.

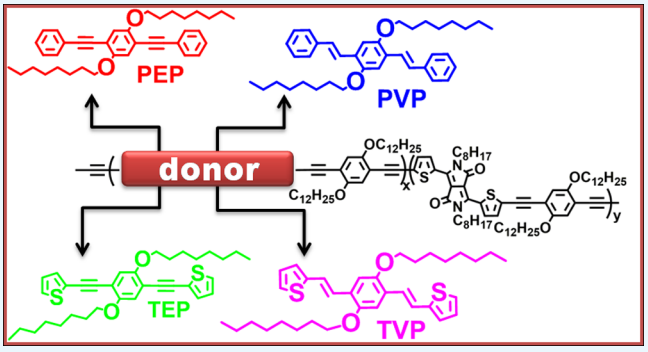

1. INTRODUCTION

In bulk heterojunction solar cell (BHJSC) devices, a donor-conjugated polymer is mixed with acceptor molecules to form an active layer where the donor polymer[1] absorbs light energy to release electrons that pass to acceptor so that the charge separation can happen to produce electrical energy. The performance of solar cell devices[2,3] often depends on the band gap of the donor polymers[4−6] because the lower band gap allows absorption of light in the broad ranges of wavelength.[7−9] Tuning of band gap is also important for the matching of the energy levels of donor and acceptor moieties for efficient transfer of electrons.[10] As per the recent literature reports, fullerenes have emerged as the material of choice for acceptor moiety; diketopyrrolopyrrole (DPP)-based polymers[11] have been established as the most promising candidate for donor material in BHJSCs.[12−15] Particularly, DPP core[16,17] has attracted a lot of attention recently because it is a fused aromatic core with a strong electron withdrawing part. It consists of two carbonyl groups to enhance intramolecular or intermolecular interactions via $\pi-\pi$ stacking of the polymer chains in solid states. Furthermore, DPP moiety is linked with other aromatic moiety by double bond or triple bond (linker) for fine tuning of electronic properties (typically, donor−acceptor or D−A type). For example, isoindigo, benzodithiophene, dithienosilole or substituted bithiophenes, and other aromatic moieties, cyclic amides and diimides have been linked.[13,18] In this context, the incorporation of thiophene moieties with properly designed conjugated D−A systems by a linker is more effective because of the electron-rich characteristics. As a linker, double bonds or triple bonds[19,20] have been extensively used to connect thiophene with different aromatic moieties. For example, Wang and Chen groups highlighted the insertion of ethylenic double bonds between heterocyclic rings such as thiophene and selenophene.[21,22] In this case, the double bond linkage affects the $\pi-\pi$ stacking distance between the polymer chain planes and enhances the charge carrier mobility. Chen et al. studied the comparison of two thiophenes in central vinylene group copolymer with DPP units for field effect transistor applications.[22] The same group extended the work with four thiophenes and a central vinylene group (double bond linker) with DPP.[23] On the other hand, Wu et al. reported the benefits of triple bond as a linker for thermal

Received: May 25, 2018
Accepted: September 3, 2018
Published: September 24, 2018

DOI: 10.1021/acsomega.8b01132
ACS Omega 2018, 3, 11710−11717

Scheme 1. Synthesis of Different DPP-Based Conjugated Homopolymers or Copolymers (P1−P5) Linked by Double Bond or Triple Bond with Various Aromatic Repeating Units Such as Phenyl or Thiophene with Varying Degrees of Polymerization[a]

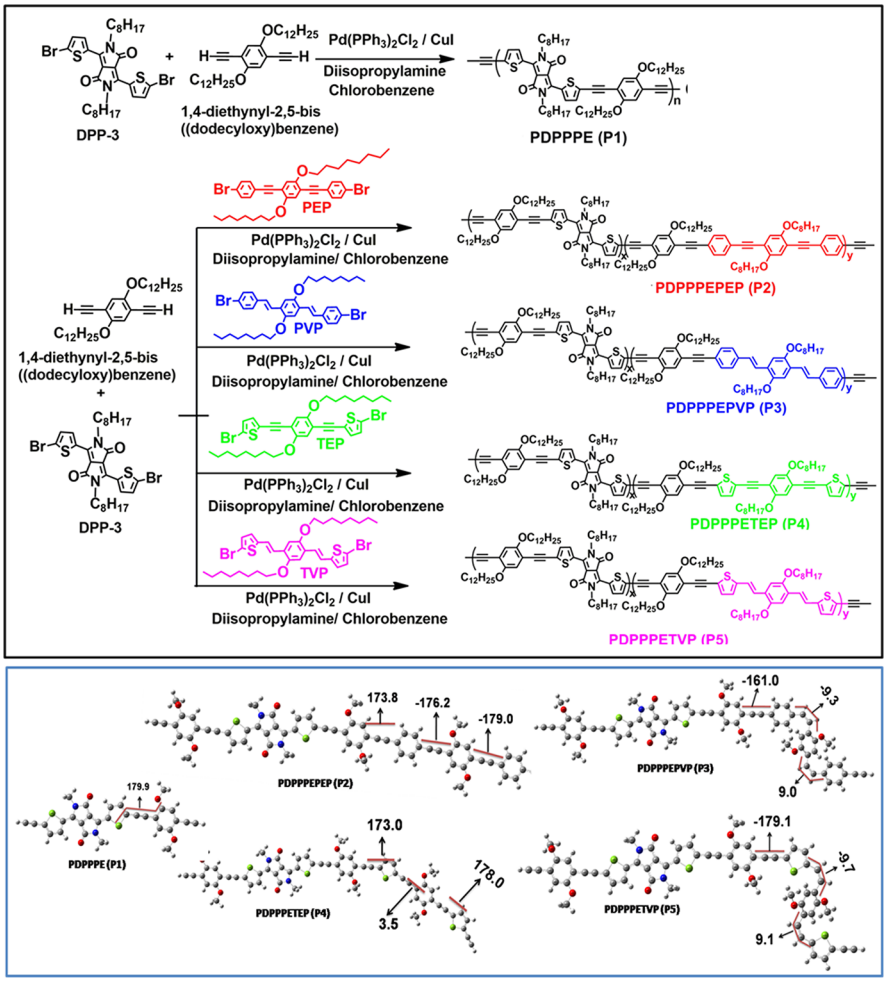

[a]Bottom inset figure shows optimized structures of the model systems at B3LYP/6-31G(d) level of theory and their corresponding dihedral angles.

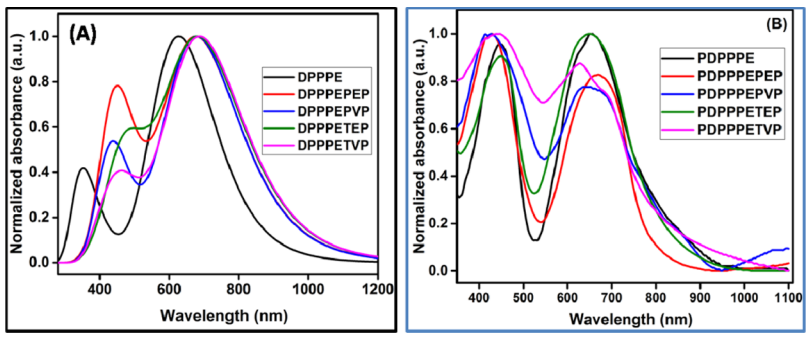

Figure 1. (A) Theoretically calculated UV−vis absorption spectra obtained by time-dependent DFT at the PBE0/6-31G* level of theory (B) UV−vis absorption spectra of the polymers (P1−P5) after fabricating as thin film on the quartz surface.

stability and photovoltaic performances in ethynyl DPP-based small molecules.[24] In this case, the weak electron withdrawing nature due to the sp-hybridized carbon atoms may lead to a lower HOMO (highest occupied molecular orbital) level, and conjugated cylinder-like π-electron density is more adaptable to conformational and steric constrains. Ouyang and others explained the importance of the triple bond linker for different polymers.[25] Hany and others reported the synthesis of N-alkylated DPP-containing compounds extended through internal double bond linker.[26]

To the best of our knowledge, there is only limited report, if any, of the detail comparative study of different DPP-based polymers linked by both double bonds and triple bonds, by theoretical and experimental investigations that could be useful for rational design of future photovoltaic devices.

In this paper, we describe the synthesis of five different DPP-based homopolymers or copolymers consisting of thiophenes and other aromatic moieties linked by triple bonds/double bonds (or both) to compare their electrochemical, optical, thermal, crystalline, and other properties and correlate with

DOI: 10.1021/acsomega.8b01132
ACS Omega 2018, 3, 11710−11717

Table 1. Theoretical and Experimental Optical Absorbance Values of Different Polymers with Various Molecular Weights

	theoretical		experimental				
polymer	λ_{max} (nm)	λ_{onset} (nm)	λ_{max} (nm) TF	λ_{onset} (nm)	M_n (g/mol)	M_w (g/mol)	PDI
PDPPPE (P1)	354, 628	894	448, 652	926	6206	12 659	2.0
PDPPPEPEP (P2)	452, 676	981	429, 670	848	3824	14 856	3.88
PDPPPEPVP (P3)	438, 679	984	427, 634	916	7350	20 064	2.73
PDPPPETEP (P4)	491, 682	1011	448, 649	908	7494	17 126	2.28
PDPPPETVP (P5)	463, 687	1011	443, 685	920	7122	23 785	3.33

theoretical calculations. All the polymers have multiple numbers of long alkyl chains[27] to render solubility in common organic solvents and to influence interchain interactions.[28,29]

Scheme 1 depicts the strategy of synthesis of those polymers using Sonogashira coupling. The optimized geometries of all the polymers obtained by computational studies are provided in the inset bottom figure of Scheme 1.

2. RESULTS AND DISCUSSION

2.1. Synthesis, Characterization, and Computational Modeling. All the monomers were synthesized by modified literature procedures, characterized by ^{1}H and ^{13}C NMR spectroscopy, and described in Supporting Information. The polymers were synthesized by Sonogashira coupling polymerization and characterized by NMR and gel permeation chromatography (GPC), and detail account is provided in Supporting Information. Geometry optimization and computational studies were performed using Gaussian 09 suit of program.

2.2. Optical Properties of the Polymers: Theoretical Predictions and Experimental Observation. Figure 1A depicts the theoretical UV−vis absorption spectra of different polymers P1, P2, P3, P4, P5 calculated at PBE0/6-31G* level of theory using Gaussian 09 suit of program,[30] and Figure 1B depicts the experimental observation of UV−vis absorption of the same polymers coated on quartz surface. In both the cases, a broad range of absorption was noticed for all the polymers covering almost the entire UV−vis range and reaching up to the near-infrared region range. This is particularly important because a wide range of absorption should ensure maximum utilization of sunlight when the device would be fabricated using those polymers. This wide range of absorption may be attributed to the presence of different chromophores, conjugated double or triple bonds and strong intermolecular interactions.[31−33] Furthermore, calculation suggested two distinct absorption bands in all the polymers, which were also experimentally observed. Both the calculation and experimental observations showed the first absorption band located at a shorter wavelength of 350−550 nm while the second strong absorption bands were located between 550 and 1100 nm which may be attributed to $\pi-\pi^*$ transition and internal charge transfer effect. Minor variations in the λ_{max} values and λ_{onset} values were observed between the computational model and experimental observations. This may be attributed to the fact that while theoretical value was calculated based on one repeating unit for the computational feasibility; all the polymers actually have multiple repeating units with a varied number of degree of polymerization. As observed from Table 1, the number average molecular weight (M_n), which depends on the degree of polymerization can influence the experimental λ_{onset} or onset value significantly. For example, it was observed from Table 1 that polymer with a minimum value of number average molecular weight (P2 with M_n value of 3824 g/mol) showed comparatively a less value of λ_{onset} in thin film at 848 nm while polymer with an M_n value of 6000−7000 g/mol showed a higher λ_{onset} value of 908−926 nm. A similar observation was noticed for λ_{max} values in solution (Supporting Information) and in thin films. This may be attributed to a large amount of extended conjugations for polymers with higher molecular weights. Moreover, the absorption was red-shifted to more than 150 nm in thin films than in solution, possibly due to strong intermolecular interactions. Furthermore, both computational calculations and experimental findings indicated that the choice of linker like double bond (polymer P3 or P5) or triple bond (P1, P2, or P4) does not significantly influence the primary optical absorption spectra.

2.3. Band Gaps of Polymers: Theoretical Prediction and Experimental Determination by the Electrochemical Method. It can be seen from frontier molecular orbital (FMO) pictures (Table 2) that both the HOMO and LUMO

Table 2. Electron Density Plots of FMOs Calculated at B3LYP/6-31G* Level of Theory

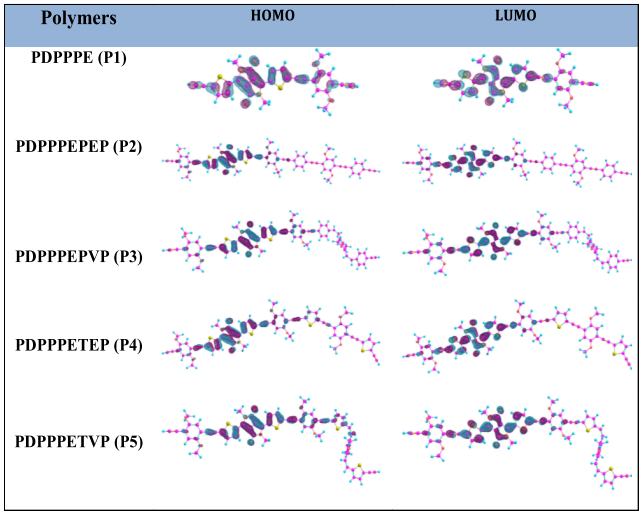

(lowest unoccupied molecular orbital) are delocalized on the DPP moiety, and all the electronic transitions appear to be $\pi-\pi^*$ in nature. The calculated HOMO−LUMO energy levels are summarized in Table 1. Computational studies indicated a minimal effect of structural variations on the band gap although theoretically predicted band gap values were lower while considering the repeating units two rather than one (Supporting Information, Table S3). However, some variation of band gaps was observed for all the polymers when HOMO, LUMO, and band gaps were determined experimentally by using cyclic voltammetry (CV) using the following equations

DOI: 10.1021/acsomega.8b01132
ACS Omega 2018, 3, 11710−11717

taking the respective onset values of oxidation and reduction states.[34] (Figure 2, Table 3).

$$\text{HOMO} = -e(E_{ox} + 4.71)\ (\text{eV})$$

$$\text{LUMO} = -e(E_{red} + 4.71)\ (\text{eV})$$

$$E_g^{ec} = e(E_{ox} - E_{red})\ (\text{eV})$$

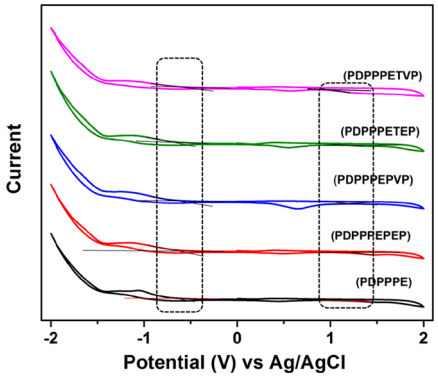

Figure 2. Cyclic voltammograms of the polymers (P1−P5) fabricated as thin films. The region inside black dotted rectangles indicates onsets of oxidation and reduction in CV curves.

In this case, it was found that the band gap was almost unchanged at 1.8 eV when the weight average molecular weight (M_w) was less than 20 000 g/mol (for P1, P2, or P4). A slight decrease of band gap to 1.7 eV was observed when the weight average molecular weight (M_w) was 20 000 (for P3) and a much lower band gap was observed at 1.5 eV when the weight average molecular weight was higher at almost 24 000 g/mol for the polymer P5. The lowering of band gaps for polymers of higher molecular weights may be attributed to a greater degree of polymerization leading to extended conjugation which was not accounted in theoretical calculations.

2.4. Characterization by Spectroscopy and GPC. Spectroscopic techniques such as ^{1}H NMR, ^{13}C NMR, and Fourier transform infrared (FT-IR) spectroscopy were used to confirm the structures of all the polymers, monomers, and all the synthesized compounds used to prepare various monomers. The ^{1}H NMR spectra of all the polymers (P1, P2, P3, P4, P5) and one of the monomers [1,4-diethynyl-2,5-bis(dodecyloxy)benzene bearing two alkyne groups] are shown in Figure 3A,B, respectively, for comparison purpose while all the other relevant ^{1}H, ^{13}C NMR spectra are provided in Supporting Information. While all the peaks in ^{1}H NMR spectra of monomers appeared sharp, usual broad peaks appeared for all the polymers because of their polydisperse

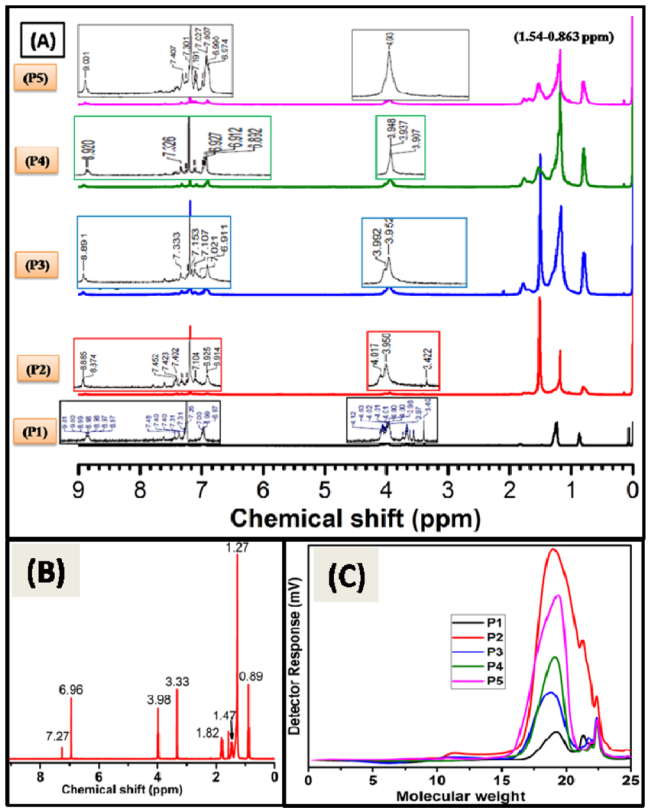

Figure 3. (A) ^{1}H NMR spectra of different polymers (P1, P2, P3, P4, P5) in $CDCl_3$. (B) ^{1}H NMR spectra of the monomer (1,4-diethynyl-2,5-bis(dodecyloxy)benzene in $CDCl_3$. (C) GPC chromatograms of the polymers in tetrahydrofuran (THF). (P1: M_n = 6206, M_w = 12 659, PDI = 2.0, P2: M_n = 7494, M_w = 17 126, PDI = 2.28, PDPPPEPVP: M_n = 7122, M_w = 23 785, PDI = 3.33, PDPPPETEP: M_n = 3824, M_w = 14 856, PDI = 3.88, PDPPPETVP: M_n = 7350, M_w = 20 064, PDI = 2.73).

nature. A characteristic peak at 3.33 ppm was observed for the monomer due to the presence of alkyne protons, which was attenuated (polymer P1 and P2) or completely disappeared (polymer P3, P4, P5) after polymerization because of effective coupling between alkynes and aromatic bromides. Slight appearance of peak at 3.33 ppm after polymerization for polymer P1 and P2 may be attributed to end alkyne groups. The signals in the range of 7.52−7.23 and 7.01−6.86 ppm are related to phenyl protons and peaks at 8.94, 7.64 ppm are assigned to DPP thiophene protons. Peaks in the range of 4.02 ppm are related to α hydrogen containing alkyl chains directly connected to the DPP-linked nitrogen atom. In the range of 6.99−7.16 ppm is the peak related to thiophene proton adjacent to alkynes in polymer PDPPPETEP-P4. In the range

Table 3. Theoretical and Experimental HOMO, LUMO, and Band Gap Values of Different Polymers

	theoretical study[a]			experimental study				
polymer	HOMO (eV)	LUMO (eV)	E_g	E_{ox}^{onset} (V)	E_{red} (V)	HOMO (eV)	LUMO (eV)	E_g^{ec} (eV)
P1	−5.01	−2.92	2.09	1.17	−0.62	−5.88	−4.08	1.8
P2	−4.91	−2.94	1.97	1.2	−0.62	−5.91	−4.09	1.82
P3	−4.91	−2.93	1.97	1.16	−0.60	−5.87	−4.11	1.76
P4	−4.90	−2.95	1.95	1.15	−0.69	−5.86	−4.02	1.84
P5	−4.89	−2.93	1.95	0.94	−0.60	−5.68	−4.11	1.54

[a]Taking into account of one repeating unit.

DOI: 10.1021/acsomega.8b01132
ACS Omega 2018, 3, 11710−11717

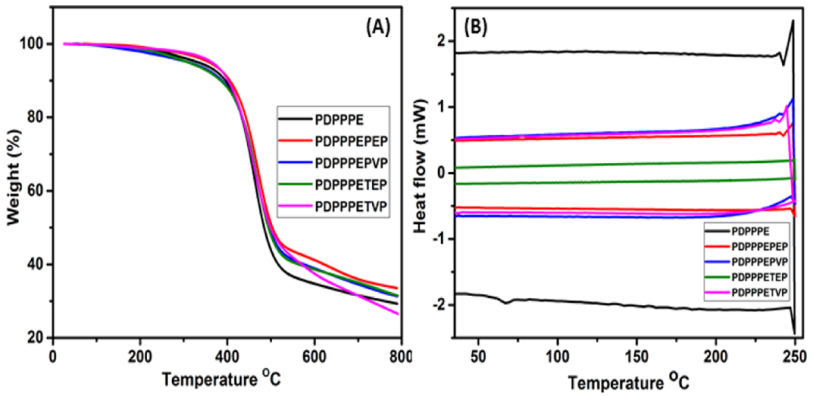

Figure 4. (A) TGA curves of the polymers recorded at a heating rate of 5 °C min^{-1} under an N_2 atmosphere (B) DSC curves of the polymers recorded at a heating rate of 10 °C min^{-1} under an N_2 atmosphere.

of 7.17−7.20 ppm is the peak for protons of internal double bond between the thiophene and phenyl ring moieties of polymer PDPPPETVP (P5).

GPC was used to evaluate the molecular weights and polydispersity of the polymers (Figure 3C). The weight average molecular weight was observed between 12 000 and 24 000 g/mol with moderate polydispersity of 2−4, indicating low to moderate degrees of polymerization in most cases. Minimum polydispersity was observed for the homopolymer, whereas polydispersity was more for the copolymers, which may be attributed to reactivity difference between the dibromide monomers.

2.5. Thermal Study. Thermal stability of all the polymers was investigated by thermogravimetric analysis (TGA), and phase transition was investigated by differential scanning calorimetry (DSC) (Figure 4A,B, respectively). The TGA analysis reveals that the onset points of the weight loss with 5% weight-loss of those polymers exhibited sufficiently high thermal decomposition temperatures (T_d-5% weight lost) with 332 °C for P1, 358 °C for P2, 310 °C for P3, 309 °C for P4 (309.09), and 364 °C for P5. This indicates that all polymers have good thermal stability, which is important for application point of view while applying for device fabrication process. Furthermore, we observed from DSC (Figure 4B) that there is no thermal transition such as melting, glass transition, or amorphous−crystalline transition between 20 and 250 °C, indicating its processability in a wide range of temperature.

2.6. Other Parameters Related to Photovoltaic Performances. The polymers were used separately for photovoltaic device fabrications, and various device parameters such as open circuit voltage (V_{oc}) and fill factors (FF) were evaluated after plotting current density−voltage (J−V) curve for all the polymers (Figure 5, inset table). The low fill factor (FF) values in most cases which may lead to low device efficacy can be attributed to appreciable extend of crystallinity of polymers as observed from X-ray diffraction (XRD) (Figure 5B), causing a phase separation during device fabrication.[35,36] The phase separations were observed in atomic force microscopy (AFM) also, which showed pondlike structures (Figure 5C) when the device architecture was simulated using donor polymer and fullerenes.

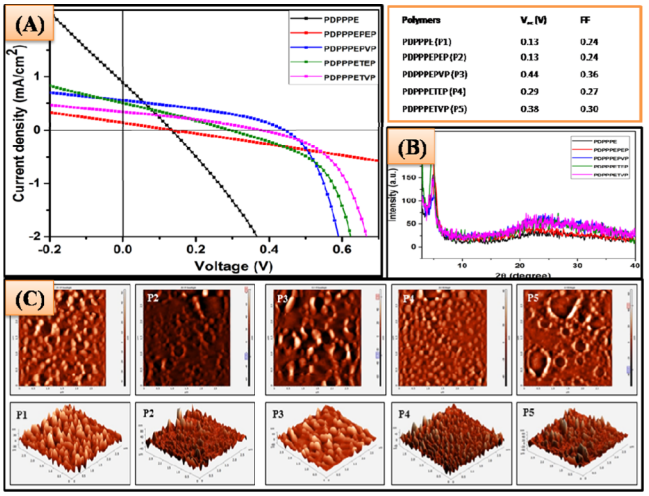

Figure 5. (A) Current density−voltage (J−V) of the bulk heterojunction photovoltaic devices fabricated using different polymers as donor component and PCBM as acceptor component. (B) XRD pattern of the polymers in powder form. (C) AFM pictures of different polymer deposited on the glass surface under simulated conditions of photovoltaic devices.

3. CONCLUSIONS

In conclusion, we have successfully used Sonogashira coupling to prepare several novel DPP-based homopolymers and copolymers with weight average molecular weights (M_w) ranging from 12 000 to 23 000 g/mol and polydispersity index (PDI) ranging from 2.0 to 3.8. Density functional theory (DFT) calculations predicted a broad range of absorption of light in the wavelength range of 300−1100 nm for all the polymers with two distinct bands at 350−500 and 550−1100 nm, respectively. Experimental UV−vis spectroscopic study on thin films corroborated this general trend. However, a dependence of experimental onset absorption value on the number average molecular weight of polymers was observed. Theoretical calculation indicated a less dependence of band gap values on nature of linkers (double or triple bond) or structure of aromatic repeating units (thiophene or benzene), while experimental determination of band gaps from CV experiments proved their dependence on weight average molecular weights. The low fill factor and open circuit voltage for the devices fabricated using those polymers may be attributed to crystallinity, nature of linkers, and other factors which might have led to low device efficacy. Those observation and theoretical calculations should be useful to design suitable polymer for improved device fabrication.

DOI: 10.1021/acsomega.8b01132
ACS Omega 2018, 3, 11710−11717

4. EXPERIMENTAL SECTION

4.1. Materials. 2-Thiophenecarbonitrile, dimethyl succinate, potassium *tert*-butoxide, 2-methyl-2-butanol, 1-bromooctane, potassium carbonate, dimethylcarbamate, *N*-bromosuccinimide, anhydrous chloroform, bistriphenylphosphine palladium(II) chloride ($Pd(PPh_3)_2Cl_2$), copper(I) iodide (CuI), 5-bromothiophene-2-carbaldehyde, ethynyltrimethylsilane, 1-bromo-4-iodobenzene, and anhydrous toluene were purchased from Sigma-Aldrich chemical company and used without any further purification. Hydroquinone, bromine, diisopropylamine (DIPA), sodium hydroxide (NaOH), sodium carbonate (Na_2CO_3), concentrated hydrochloric acid (concd HCl), dimethylformamide, potassium carbonate (K_2CO_3), THF, methanol, toluene, dichloromethane, ethyl acetate, and pet ether were purchased from Merck.

4.2. Instrumental Details. A Bruker 400 MHz NMR spectrometer was used to record the chemical shift values in ppm and *J* values in Hz. Varian Cary 50 Bio was used for UV−visible spectroscopy, while a CHI 600D electrochemical workstation was used for CV using ferrocene/ferrocenium ion (Fc/Fc+) redox couple as the external standard with a potential of 0.09 eV against (Ag/Ag^+) potential. The GPC was performed using a Viscotek VE 1122 pump, a Viscotek VE 3580 RI detector, and a Viscotek VE 3210 UV−vis detector in THF using polystyrene as standards. TGA data were obtained from Mettler Toledo TGA/SDTA 851e, and DSC data were recorded using a DSC instrument with a heating rate of 5 °C min^{-1} in a nitrogen atmosphere. AFM data were recorded on a Nova 1.0.26 RC1 atomic force microscope in semicontact mode with NT-MDT solver software in Advanced Materials Lab. XRD data for polymers were obtained using a Bruker AXS D8 advance X-ray diffractometer in Advanced Materials Lab.

4.3. Computational Study. DFT-based quantum chemical calculations were applied to gain the molecular level understanding of the observed electronic and optical properties of the systems. All calculations were carried out using Gaussian 09 suite of program. To model the synthesized compounds, monomeric units of donor−acceptor systems of repeating terpolymers were considered. Geometries of all the five model systems were optimized at B3LYP/6-31G* level of theory. The geometry optimization was carried out without any symmetry constraints. The solvent effect was included using polarizable continuum model of solvation. It was also ensured that the obtained vibrational frequencies were real, therefore corresponded to true minima on the potential energy function.

4.4. Device Architecture: Fabrication and Characterization of Photovoltaic Cells. The indium tin oxide (ITO)-coated glass substrates were cleaned sequentially with deionized water, acetone, and 2-propanol in an ultrasound bath for 20 min each and then dried at 70 °C for overnight. The general organic photovoltaic device architecture of (ITO)/polymer:[6,6]-phenylC_{71}-butyric acid methyl ester/LiF/Al configuration and the hole transport material poly-(3,4-ethylenedioxythiophene)−poly-(styrenesulfonate) (PEDOT−PSS) Clevios PH solution was spin-coated onto the clean ITO substrates at 5000 rpm, followed by annealing at 130 °C for 15 min in ambient conditions to give a thickness of ∼40 nm. BHJ devices based an active layer blend were prepared by dissolving the polymers and [6,6]-phenyl C_{61}-butyric acid methyl ester (PCBM) in 1,2-dichlorobenzene with different D−A weight ratios with the weight ratio of 1:1.5 (16 mg/mL). The mixed solution was spin-coated onto the top of the PEDOT−PSS layer at 1000 rpm for 60 s and then dried at room temperature for 30 min. The thickness of the active layer is about 100 ± 5 nm. Finally, 1 nm of LiF electron extraction layer was deposited on the active layer. As LiF may reduce the work function of cathode also preventing Al diffusion into the active layer which is leading to efficient electron extraction followed by Al top electrode was deposited onto the top of LiF by thermal evaporation under high vacuum condition (10^{-6} Torr). The active area of the devices was found to be 0.08 cm^2. The device characterization was carried out under an inert condition (Ar-filled glovebox) using an AM 1.5G solar simulator with an irradiation intensity of 80 mW/cm^2.

4.5. General Procedure for Polymerization. To a hot gun-dried 25 mL two neck round bottom flasks, we added dibromo compounds (DPP3, PEP, PVP, TEP, or TVP) and dialkyne compound [3D-1,4-diethynyl-2,5-bis((dodecyloxy)-benzene)] along with 10 mol percentage $Pd(PPh_3)_2Cl_2$ and 20 mol percentage CuI in N_2 purged mixture of solvent (chlorobenzene + DIPA). The reaction mixture was again degassed with N_2 gas, and the reaction medium was maintained at 70 °C for 48 h under an N_2 atmosphere. After completion of polymerization, the crude polymer was purified with Soxhlet, extracted with hot methanol, hexane, and acetone to remove the monomers and oligomer impurities to obtain pure blue color polymer fraction from chloroform and chlorobenzene.

4.6. Synthesis of PDPPPE (P1). Following the general procedure for polymerization using DPP3 (200 mg, 0.292 mmol), 1,4-diethynyl-2,5-bis((dodecyloxy)benzene) (144 mg, 0.292 mmol), and an N_2 purged mixture of solvent (12 mL chlorobenzene and 5 mL DIPA), $Pd(PPh_3)_2Cl_2$ (40 mg, 0.058 mmol), and CuI (6 mg, 0.058 mmol), a dark blue color polymer from chloroform and chlorobenzene fraction (Soxhlet extraction) was obtained. Total 220 mg. GPC: (M_w = 12 659, PDI = 2.0). ^{1}H NMR (400 MHz, $CDCl_3$): δ 8.94 (s), 7.64 (d), 7.52−7.23 (m), 7.01−6.86 (m), 4.13−3.92 (m), 3.39 (s), 1.37 (dd), 1.84 (br d), 1.26 (br s), 0.86 (br s).

4.7. Synthesis of PDPPPEPEP (P2). Following the general procedure for polymerization using DPP3 (100 mg, 0.146 mmol), PEP (103 mg, 0.146 mmol), 1,4-diethynyl-2,5-bis((dodecyloxy)benzene) (144 mg, 0.292 mmol), and an N_2 purged mixture of solvent (12 mL chlorobenzene + DIPA 7 mL), $Pd(PPh_3)_2Cl_2$ (20 mg, 0.058 mmol), and CuI (11 mg, 0.058 mmol), a dark pure blue color polymer fraction (220 mg) from Soxhlet extraction was obtained. GPC: (M_n = 7494, M_w = 17 126, PDI = 2.28). ^{1}H NMR (400 MHz, $CDCl_3$): δ 8.92 (br m), 7.66 (d), 7.52 (br m), 5.40 (br m), 7.19 (br m), 7.0 (br m), 4.02 (br d), 1.84 (br d), 1.26 (br s), 0.86 (br s).

4.8. Synthesis of PDPPPEPVP (P3). Following the general procedure for polymerization using DPP3 (100 mg, 0.146 mmol), PVT (101 mg, 0.146 mmol), 1,4-diethynyl-2,5-bis((dodecyloxy)benzene) (144 mg, 0.292 mmol), and an N_2 purged mixture of solvent (8 mL chlorobenzene + DIPA 8 mL), $Pd(PPh_3)_2Cl_2$ (20 mg, 0.0292 mmol), and CuI (11 mg, 0.058 mmol), a dark blue color polymer fraction (198 mg) from Soxhlet extraction was obtained after solvent evaporation. GPC: (M_n = 7122, M_w = 23 785, PDI = 3.33). ^{1}H NMR (400 MHz, $CDCl_3$): δ 8.98−8.78 (br m), 7.59 (br m), 7.40−7.22 (br m), 7.22−6.96 (br m), 6.91 (br s), 4.02 (br m), 1.84 (br d), 1.61 (br m), 1.38−0.88 (br m), 0.81 (t).

4.9. Synthesis of PDPPPETEP (P4). Following the general procedure for polymerization using (DPP3 100 mg, 0.146 mmol), TEP (103 mg, 0.146 mmol), 1,4-diethynyl-2,5-

DOI: 10.1021/acsomega.8b01132
ACS Omega 2018, 3, 11710−11717

bis((dodecyloxy)benzene) (144 mg, 0.292 mmol), and an N_2 purged mixture of solvent (8 mL chlorobenzene + DIPA 8 mL), $Pd(PPh_3)_2Cl_2$ (20 mg, 0.0292 mmol), and CuI (11 mg, 0.058 mmol), a dark blue color polymer fraction (215 mg) from Soxhlet extraction after solvent evaporation was obtained. GPC: (M_n = 3824, M_w = 14 856, PDI = 3.88). ^{1}H NMR (400 MHz, $CDCl_3$): δ 8.92 (s), 7.49−7.36 (m), 7.33 (s), 7.21 (d), 7.09 (s), 6.92 (br dd), 4.02 (t), 1.84 (br d), 1.60 (br m), 1.35−0.87 (br m), 0.79 (d).

4.10. Synthesis of PDPPPETVP (P5). Following the general procedure for polymerization using DPP3 (100 mg, 0.146 mmol), TVP (103 mg, 0.146 mmol), 1,4-diethynyl-2,5-bis((dodecyloxy)benzene) (144 mg, 0.292 mmol), and an N_2 purged mixture of solvent (8 mL chlorobenzene + DIPA 8 mL), $Pd(PPh_3)_2Cl_2$ (20 mg, 0.0292 mmol), and CuI (11 mg, 0.058 mmol), a dark blue color polymer fraction (182 mg) from Soxhlet after solvent evaporation was obtained. GPC: (M_n = 7350, M_w = 20 064, PDI = 2.73). ^{1}H NMR (400 MHz, $CDCl_3$): δ 9.01 (br s), 7.37−7.05 (br m), 7.05−6.74 (m), 4.04 (br m), 1.85 (br d), 1.58−1.24 (br m), 0.86 (d).

■ ASSOCIATED CONTENT

Supporting Information

The Supporting Information is available free of charge on the ACS Publications website at DOI: 10.1021/acsomega.8b01132.

PEP, PVP, TEP, PVP, DPP1, DPP2, DPP3 monomers and their intermediates' synthetic procedure, spectroscopic (^{1}H, ^{13}C, DEPT NMR, FT-IR, and UV−visible) analysis, microscopic analysis (AFM), thermal analysis (TGA & DSC), molecular weight determination (GPC method), morphology analysis (XRD), and optimized structure and theoretical prediction (Gaussian 09 suite of program) (PDF)

■ AUTHOR INFORMATION

Corresponding Authors

*E-mail: subbu@clri.res.in, subuchem@hotmail.com. Phone: +91-44-24422059, +91 44 24411630. Fax: + 91-44-24911589 (V.S.).

*E-mail: debasis@clri.res.in, debasis.samanta@gmail.com. Phone: +91-44-24437189. Fax: + 91-44-24911589 (D.S.).

ORCID

Kothandam Krishnamoorthy: 0000-0003-0603-8694

Asit Baran Mandal: 0000-0001-7953-941X

Venkatesan Subramanian: 0000-0003-2463-545X

Debasis Samanta: 0000-0002-3043-8033

Notes

The authors declare no competing financial interest.

■ ACKNOWLEDGMENTS

P.M. acknowledges CSIR, Government of India, and V.R. acknowledges DST (INSPIRE scheme) for the support in the form of Senior Research Fellowship. Support from CSIR-TAPSUN is acknowledged. We are thankful to Dr. N. Somanathan, former head, Polymer Department, CSIR-CLRI for valuable discussions, encouragement, and support. A.B.M. is also grateful to the Indian National Academy of Engineering (INAE) and CSIR-CGCRI, Kolkata, for INAE Distinguished Professorship. Financial support from DST project (ECR/2015/000219) is gratefully acknowledged. CSIR-CLRI communication No. A/2018/PLY/CSIR-DST/1281.

■ REFERENCES

(1) Nielsen, C. B.; Turbiez, M.; McCulloch, I. Recent Advances in the Development of Semiconducting DPP-Containing Polymers for Transistor Applications. *Adv. Mater.* **2013**, *25*, 1859−1880.

(2) Lu, L.; Zheng, T.; Wu, Q.; Schneider, A. M.; Zhao, D.; Yu, L. Recent Advances in Bulk Heterojunction Polymer Solar Cells. *Chem. Rev.* **2015**, *115*, 12666−12731.

(3) Zhan, X.; Zhu, D. Conjugated polymers for high-efficiency organic photovoltaics. *Polym. Chem.* **2010**, *1*, 409−419.

(4) Roth, B.; Savagatrup, S.; de los Santos, N. V.; Hagemann, O.; Helgesen, M.; Carlé, J. E.; Livi, F.; Bundgaard, E.; Søndergaard, R. R.; Krebs, F. C.; Lipomi, D. J. Mechanical Properties of a Library of Low-Band-Gap Polymers. *Chem. Mater.* **2016**, *28*, 2363−2373.

(5) Liu, C.; Wang, K.; Gong, X.; Heeger, A. J. Low bandgap semiconducting polymers for polymeric photovoltaics. *Chem. Soc. Rev.* **2016**, *45*, 4825−4846.

(6) Kim, J.-H.; Song, C. E.; Kim, B. S.; Kang, I.-N.; Shin, W. S.; Hwang, D.-H. Thieno[3,2-b]thiophene-Substituted Benzo[1,2-b:4,5-b′]dithiophene as a Promising Building Block for Low Bandgap Semiconducting Polymers for High-Performance Single and Tandem Organic Photovoltaic Cells. *Chem. Mater.* **2014**, *26*, 1234−1242.

(7) Low, J. Z.; Neo, W. T.; Ye, Q.; Ong, W. J.; Wong, I. H. K.; Lin, T. T.; Xu, J. Low Band-Gap Diketopyrrolopyrrole-Containing Polymers for Near Infrared Electrochromic and Photovoltaic Applications. *J. Polym. Sci., Part A: Polym. Chem.* **2015**, *53*, 1287−1295.

(8) Dou, L.; Chang, W.-H.; Gao, J.; Chen, C.-C.; You, J.; Yang, Y. A Selenium-Substituted Low-Bandgap Polymer with Versatile Photovoltaic Applications. *Adv. Mater.* **2013**, *25*, 825−831.

(9) Huo, L.; Guo, X.; Zhang, S.; Li, Y.; Hou, J. PBDTTTZ: A Broad Band Gap Conjugated Polymer with High Photovoltaic Performance in Polymer Solar Cells. *Macromolecules* **2011**, *44*, 4035−4037.

(10) Li, W.; Roelofs, W. S. C.; Wienk, M. M.; Janssen, R. A. J. Enhancing the Photocurrent in Diketopyrrolopyrrole-Based Polymer Solar Cells via Energy Level Control. *J. Am. Chem. Soc.* **2012**, *134*, 13787−13795.

(11) Dhbaibi, K.; Favereau, L.; Srebro-Hooper, M.; Jean, M.; Vanthuyne, N.; Zinna, F.; Jamoussi, B.; Di Bari, L.; Autschbach, J.; Crassous, J. Exciton coupling in diketopyrrolopyrrole-helicene derivatives leads to red and near-infrared circularly polarized luminescence. *Chem. Sci.* **2018**, *9*, 735−742.

(12) Bronstein, H.; Chen, Z.; Ashraf, R. S.; Zhang, W.; Du, J.; Durrant, J. R.; Shakya Tuladhar, P.; Song, K.; Watkins, S. E.; Geerts, Y.; Wienk, M. M.; Janssen, R. A. J.; Anthopoulos, T.; Sirringhaus, H.; Heeney, M.; McCulloch, I. Thieno[3,2-b]thiophene−Diketopyrrolopyrrole-Containing Polymers for High-Performance Organic Field-Effect Transistors and Organic Photovoltaic Devices. *J. Am. Chem. Soc.* **2011**, *133*, 3272−3275.

(13) SambathKumar, B.; Shyam Vinod Kumar, P.; Deepakrao, F. S.; Kumar Iyer, S. S.; Subramanian, V.; Datt, R.; Gupta, V.; Chand, S.; Somanathan, N. Two Donor-One Acceptor Random Terpolymer Comprised of Diketopyrrolopyrrole Quaterthiophene with Various Donor π-Linkers for Organic Photovoltaic Application. *J. Phys. Chem. C* **2016**, *120*, 26609−26619.

(14) Ko, E. Y.; Park, G. E.; Lee, D. H.; Um, H. A.; Shin, J.; Cho, M. J.; Choi, D. H. Enhanced Performance of Polymer Solar Cells Comprising Diketopyrrolopyrrole-Based Regular Terpolymer Bearing Two Different π-Extended Donor Units. *ACS Appl. Mater. Interfaces* **2015**, *7*, 28303−28310.

(15) Bronstein, H.; Collado-Fregoso, E.; Hadipour, A.; Soon, Y. W.; Huang, Z.; Dimitrov, S. D.; Ashraf, R. S.; Rand, B. P.; Watkins, S. E.; Tuladhar, P. S.; Meager, I.; Durrant, J. R.; McCulloch, I. Thieno[3,2-b]thiophene-diketopyrrolopyrrole Containing Polymers for Inverted Solar Cells Devices with High Short Circuit Currents. *Adv. Funct. Mater.* **2013**, *23*, 5647−5654.

DOI: 10.1021/acsomega.8b01132
ACS Omega 2018, 3, 11710−11717

(16) Dhar, J.; Mukhopadhay, T.; Yaacobi-Gross, N.; Anthopoulos, T. D.; Salzner, U.; Swaraj, S.; Patil, S. Effect of Chalcogens on Electronic and Photophysical Properties of Vinylene-Based Diketopyrrolopyrrole Copolymers. *J. Phys. Chem. B* **2015**, *119*, 11307−11316.
(17) Ohta, K.; Tokonami, S.; Takahashi, K.; Tamura, Y.; Yamada, H.; Tominaga, K. Probing Charge Carrier Dynamics in Porphyrin-Based Organic Semiconductor Thin Films by Time-Resolved THz Spectroscopy. *J. Phys. Chem. B* **2017**, *121*, 10157−10165.
(18) Yu, H.; Park, K. H.; Song, I.; Kim, M.-J.; Kim, Y.-H.; Oh, J. H. Effect of the alkyl spacer length on the electrical performance of diketopyrrolopyrrole-thiophene vinylene thiophene polymer semiconductors. *J. Mater. Chem. C* **2015**, *3*, 11697−11704.
(19) Murugan, P.; Ananthakrishnan, S. J.; Somanathan, N.; Samanta, D.; Mandal, A. B. Nanoscale functionalization of surfaces by graft-through Sonogashira polymerization. *RSC Adv.* **2015**, *5*, 4121−4125.
(20) Murugan, P.; Krishnamurthy, M.; Jaisankar, S. N.; Samanta, D.; Mandal, A. B. Controlled decoration of the surface with macromolecules: polymerization on a self-assembled monolayer (SAM). *Chem. Soc. Rev.* **2015**, *44*, 3212−3243.
(21) Li, H.; Wang, X.; Liu, F.; Fu, H. High performance quinacridone-based polymers in film transistors and photovoltaics: effects of vinylene linkage on crystallinity and morphology. *Polym. Chem.* **2015**, *6*, 3283−3289.
(22) Chen, H.; Guo, Y.; Yu, G.; Zhao, Y.; Zhang, J.; Gao, D.; Liu, H.; Liu, Y. Highly π-Extended Copolymers with Diketopyrrolopyrrole Moieties for High-Performance Field-Effect Transistors. *Adv. Mater.* **2012**, *24*, 4618−4622.
(23) Liu, X.; Huang, J.; Xu, J.; Gao, D.; Zhang, W.; Shi, K.; Yu, G. Highly planar thieno[3,2-b]thiophene-diketopyrrolopyrrole-containing polymers for organic field-effect transistors. *RSC Adv.* **2016**, *6*, 35394−35401.
(24) Wu, Z.; Li, A.; Fan, B.; Xue, F.; Adachi, C.; Ouyang, J. Phenanthrene-functionalized 3,6-dithiophen-2-yl-2,5- dihydropyrrolo-[3,4-c]pyrrole-1,4-diones as donor molecules for solution-processed organic photovoltaic cells. *Sol. Energy Mater. Sol. Cells* **2011**, *95*, 2516−2523.
(25) Wu, Z.; Fan, B.; Li, A.; Xue, F.; Ouyang, J. Low-band gap copolymers of ethynylfluorene and 3,6-dithiophen-2-yl-2,5-dihydropyrrolo[3,4-c]pyrrole-1,4-dione synthesized under microwave irradiation for polymer photovoltaic cells. *Org. Electron.* **2011**, *12*, 993−1002.
(26) Kylberg, W.; Sonar, P.; Heier, J.; Tisserant, J.-N.; Müller, C.; Nüesch, F.; Chen, Z.-K.; Dodabalapur, A.; Yoon, S.; Hany, R. Synthesis, thin-film morphology, and comparative study of bulk and bilayer heterojunction organic photovoltaic devices using soluble diketopyrrolopyrrole molecules. *Energy Environ. Sci.* **2011**, *4*, 3617−3624.
(27) Peteanu, L. A.; Chowdhury, S.; Wildeman, J.; Sfeir, M. Y. Exciton-Exciton Annihilation as a Probe of Interchain Interactions in PPV-Oligomer Aggregates. *J. Phys. Chem. B* **2017**, *121*, 1707−1714.
(28) Chung, K.; McAllister, A.; Bilby, D.; Kim, B.-G.; Kwon, M. S.; Kioupakis, E.; Kim, J. Designing interchain and intrachain properties of conjugated polymers for latent optical information encoding. *Chem. Sci.* **2015**, *6*, 6980−6985.
(29) Lee, C.-H.; Lai, Y.-Y.; Hsu, J.-Y.; Huang, P.-K.; Cheng, Y.-J. Side-chain modulation of dithienofluorene-based copolymers to achieve high field-effect mobilities. *Chem. Sci.* **2017**, *8*, 2942−2951.
(30) Vijay, D.; Varathan, E.; Subramanian, V. Theoretical design of core modified (oxa and thia) porphyrin based organic dyes with bridging thiophene linkers. *J. Mater. Chem. A* **2013**, *1*, 4358−4369.
(31) Wang, H.; Ding, Y.; Lai, Y.; Sun, Z.; Liu, Y.; Jiang, B.; Chen, M.; Yao, J.; Liu, F.; Russell, T. P. Ethynylene-linked benzo[1,2-b:4,5-b′]dithiophene-alt-diketopyrrolopyrrole alternating copolymer: optoelectronic properties, film morphology and photovoltaic applications. *J. Mater. Chem. A* **2015**, *3*, 12972−12981.
(32) Kan, Y.; Liu, C.; Zhang, L.; Gao, K.; Liu, F.; Chen, J.; Cao, Y. Solution-processed small molecules with ethynylene bridges for highly efficient organic solar cells. *J. Mater. Chem. A* **2016**, *4*, 14720−14728.
(33) An, T. K.; Kang, I.; Yun, H.-j.; Cha, H.; Hwang, J.; Park, S.; Kim, J.; Kim, Y. J.; Chung, D. S.; Kwon, S.-K.; Kim, Y.-H.; Park, C. E. Solvent Additive to Achieve Highly Ordered Nanostructural Semicrystalline DPP Copolymers: Toward a High Charge Carrier Mobility. *Adv. Mater.* **2013**, *25*, 7003−7009.
(34) Hou, J.; Tan, Z.; Yan, Y.; He, Y.; Yang, C.; Li, Y. Synthesis and photovoltaic properties of two-dimensional conjugated polythiophenes with bi(thienylenevinylene) side chains. *J. Am. Chem. Soc.* **2006**, *128*, 4911−4916.
(35) Sonar, P.; Foong, T. R. B.; Singh, S. P.; Li, Y.; Dodabalapur, A. A furan-containing conjugated polymer for high mobility ambipolar organic thin film transistors. *Chem. Commun.* **2012**, *48*, 8383−8385.
(36) Shahid, M.; McCarthy-Ward, T.; Labram, J.; Rossbauer, S.; Domingo, E. B.; Watkins, S. E.; Stingelin, N.; Anthopoulos, T. D.; Heeney, M. Low band gap selenophene-diketopyrrolopyrrolepolymers exhibiting high and balanced ambipolar performance in bottom-gate transistors. *Chem. Sci.* **2012**, *3*, 181−185.

DOI: 10.1021/acsomega.8b01132
ACS Omega 2018, 3, 11710−11717